Journal of Catalysis **203,** 1–6 (2001)
doi:10.1006/jcat.2001.3389, available online at http://www.idealibrary.com on IDEAL®

PRIORITY COMMUNICATION

Methanol Electrooxidation on Platinum/Ruthenium Nanoparticle Catalysts

P. Waszczuk,* J. Solla-Gullón,† H.-S. Kim,* Y. Y. Tong,* V. Montiel,† A. Aldaz,† and A. Wieckowski*,[1]

*Department of Chemistry, University of Illinois at Urbana-Champaign, Urbana, Illinois 61801; and †Department of Physical Chemistry, University of Alicante, Apt. 99, 03080 Alicante, Spain

Received July 25, 2001; accepted August 8, 2001

Using the spontaneous deposition method (W. Chrzanowski and A. Wieckowski, *Langmuir* 13, 5974 (1997)), platinum nanoparticles were decorated with ruthenium to obtain a Pt/Ru catalyst with a packing density of up to 0.65 Ru atoms per Pt surface atom. The activity of this catalyst toward methanol electrooxidation was tested at electrode potentials of interest for fuel cells. The catalyst activity maximizes at ruthenium packing density 0.4–0.5, and the catalyst is twice as active (displays higher current densities normalized to real surface area) as the commercial 50 : 50 Pt/Ru alloy catalyst. Hydrogen adsorption on the decorated Pt/Ru and Pt/Ru alloy surfaces is also reported. © 2001 Academic Press

Key Words: **electrocatalysis; fuel cells; nanoparticle; anode; methanol.**

INTRODUCTION

The direct oxidation methanol fuel cell (DMFC) is a promising future energy technology alternative to conventional energy-generating devices because of its high energy conversion efficiency, low-to-zero pollutant emission, methanol fuel availability, ease in distribution, and high energy density of the fuel (1). A typical DMFC anode, where methanol oxidation occurs, contains a platinum-based nanoparticle catalyst, unsupported or supported, which can be deposited on a proton exchange membrane, the solid electrolyte of the cell (2). Platinum is used because of its activity in methanol activation (3), namely the C–H bond break followed by several fast steps completed by either surface CO or dissolved CO_2 formation (4). To avoid deleterious poisoning of platinum by the chemisorbed CO, or to improve platinum tolerance of chemisorbed CO, the CO needs to be removed from the surface by oxidation to CO_2. Such an oxidation process is slow on the Pt catalyst alone at potentials attractive to DMFC applications, namely, not exceeding 0.4 vs SHE (Standard Hydrogen Electrode). To improve the tolerance, transition metals like ruthenium are incorporated into the Pt catalyst and enhance catalysis by promoting activation of water and facilitate the concomitant transfer of oxygen to CO on its way to CO_2 (the bifunctional mechanism (3, 5–7); also, reactions 2 and 3 in this report). The electronic modification by a so-called ligand mechanism involved in the catalytic enhancement is also considered (8–10).

In this communication, we produced nanoparticle Pt/Ru catalyst using spontaneous deposition of ruthenium (11) on commercial platinum nanoparticles, monitored its activity toward methanol oxidation, and compared the activity to that of commercial, Johnson Matthey Pt/Ru alloy nanoparticle catalyst. The Johnson Matthey Pt/Ru catalyst was prescreened for high activity (12) and may be considered a representative benchmark for high-class commercial products of the Pt/Ru-type alloy catalyst. The spontaneous deposition involves immersing platinum in ruthenium chloride solution, flushing the cell with supporting electrolyte, and breaking galvanically the chemisorbed Ru-containing precursors to metallic/oxide ruthenium forms (11). The method has several important advantages vs other approaches. It is simple, yields structurally heterogeneous surfaces decorated by nanosized islands of predominantly monoatomic heights, and provides an excellent way for adjusting ruthenium coverage on platinum in a submonolayer deposition regime. In this communication, using steady-state methanol oxidation current measurements, we demonstrate that the catalytic activity of the decorated Pt/Ru catalyst is much higher than that of the commercial Pt/Ru alloy catalyst. Mechanistic aspects of our observations are discussed, and the capability of our synthetic approach in the field of heterogeneous electrocatalysis for fuel cells is highlighted.

EXPERIMENTAL

A conventional three-electrode electrochemical cell was used for the measurements, with a high-surface-area Pt

[1] To whom correspondence should be addressed at Department of Chemistry, University of Illinois, Box 56-5, 600 S. Mathews, Urbana, Illinois 61801. Fax: (217) 244-8068. E-mail: andrzej@scs.uiuc.edu.

0021-9517/01 $35.00

gauze as the counter electrode and the Ag/AgCl in 3 M NaCl reference (all potentials in this paper are quoted vs the SHE electrode), powered by a PGP201 Potentiostat/Galvanostat (Radiometer). The working electrode was made of the Pt and Rt/Ru catalyst immobilized on a surface of a gold disc (12 mm in diameter, 8 mm in height). The procedure for electrode fabrication (13) involved, *first*, the preparation of a suspension of a known amount of Pt powder in Millipore water; *second*, placing an aliquot of the suspension (typically 100 μl at 4 mg/ml of the catalyst) on a gold disk; *third*, air-drying of the suspension to yield a uniform thin film of the catalyst. The application of this procedure permits easy control of catalyst loading and, apparently, the nanostructured electrodes prepared this way are stable upon electrochemical performance, easily withstand purging the solution with inert or reactive (CO) gasses, and the electrolyte exchange. Notice that gold is inactive in a methanol decomposition process and serves only as a conducting inert support for the catalyst (13). Some measurements were also conducted using the catalysts sedimented on a bottom of a gold boat, as published before (12). All measurements were carried out at room temperature.

Johnson & Matthey Pt black catalyst (ca. 10 nm diameter, 20 $m^2\ g^{-1}$) was used as a substrate for deposition of Ru adlayers. A 50 : 50 Pt/Ru alloy catalyst (Johnson & Matthey Pt/Ru black, ca. 2.5 nm diameter, 65 $m^2\ g^{-1}$ as specified by the manufacturer) was used as the standard for the comparison with the methanol oxidation activity of the decorated catalyst (see Introduction). The 0.5 M H_2SO_4 supporting electrolyte was prepared from concentrated analytical grade sulfuric acid from Mallinckrodt Baker (Paris, KT) diluted in Millipore water. Ultra high purity argon gas was used to deaerate the cell. Methanol was ACS grade (Fisher Scientific), and other solutions were made of $HClO_4$ (GFS Chemicals) and $RuCl_3$ (Alfa AESAR) chemicals.

RESULTS

Platinum black immobilized on the gold substrate was used either as the catalyst itself or as a building block of the catalyst obtained by spontaneous deposition of ruthenium on platinum (Figs. 1 and 2). In the latter case, a sample of Pt black was cleaned by holding it at 0.45 V in 0.1 M $HClO_4$ and transferred to a clean beaker, which was followed by spontaneous deposition of ruthenium from 1 mM $RuCl_3$ in 0.1 M $HClO_4$ solution at open circuit potential (ca. 1 V), for 1 h. The particle catalyst was washed off with Millipore water and placed into the cell at an open circuit potential, and the potential was stepped to 0.3 V to reduce the adsorbed Ru precursor to metallic Ru (11, 14). A portion of the sample was taken for the electrochemical measurements, and the remainder of the sample was used for the electrode surface area determination, see below. Once the Pt surface decorated by metallic ruthenium (14) was obtained in the first

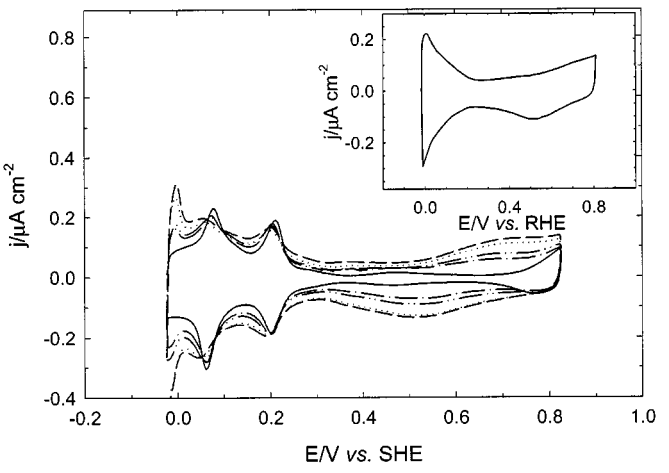

FIG. 1. Cyclic voltammogram of Pt (- - - -) and Pt/Ru after: 1st (- - · –), 2nd (- - · · –), 3rd (· · · ·), and 4th (– –) spontaneous deposition of ruthenium at the Ru packing density 0.00 (the clean Pt electrode); 0.20, 0.25, 0.35, and 0.40, respectively. Ruthenium was deposited from 1 mM $RuCl_3 + 0.1$ M $HClO_4$ for 1 h (see text). The supporting electrolyte was 0.5 M H_2SO_4, and the scan rate was 10 mV min^{-1}. The inset shows a cyclic voltammogram for the Pt/Ru commercial alloy catalyst at 20 mV min^{-1}.

deposition, the spontaneous deposition could be repeated as many times as needed in order to obtain the desired Ru packing density, e.g., up to four times in this project.

For each of the three catalysts, the real surface area was determined as follows. For the Pt catalyst, the surface area was calculated from the hydrogen deposition charge, assuming the number of surface sites on the Pt electrode (Γ_{Pt}) equal to 1.3×10^{15} Pt atoms cm^{-2}, and the 1 : 1 ratio between a Pt site and an adsorbed hydrogen atom, as routinely made (15). Since the mass of the Pt sample was also known, the

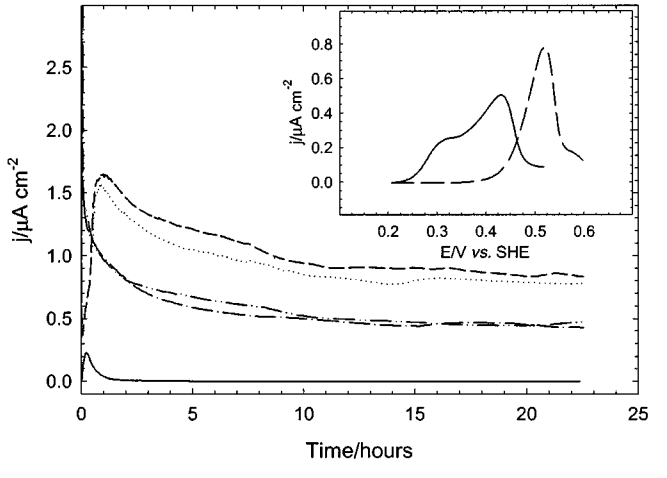

FIG. 2. Methanol oxidation current density on Pt (—) and Pt/Ru after 1st (– · –), 2nd (– · · –), 3rd (· · · ·), and 4th (– –) deposition in 0.5 M methanol and 0.5 M H_2SO_4 solution (see Fig. 1). The inset shows CO stripping voltammograms for the clean Pt electrode (the dashed line), and for the decorated Pt/Ru surface (the solid line).

specific surface area of the catalyst, S (in $cm^2\ g^{-1}$), was easily obtained. The same procedure was used for measurements of the surface area for the Pt/Ru decorated surfaces (Ru spontaneously deposited onto Pt surface forms islands on top of platinum (16) and does not change the distribution of Pt surface substrate sites; see below). For the Johnson Matthey 50 : 50 Pt/Ru alloy catalyst, the total number of surface sites (collectively, both Pt and Ru) was obtained from the CO stripping charge of adsorbed CO monolayer produced from CO saturated solutions (assuming 420 $\mu C\ cm^{-2}$ for CO oxidation (17)). Notably, when the decorated Pt/Ru catalyst was tested by the CO stripping method, the surface area was the same as obtained from the Pt hydrogen deposition method alone. This confirms indirectly that the ratio between surface sites and CO molecules is very nearly 1 : 1.

For measurements of ruthenium packing density on the decorated catalysts, a Pt/Ru sample was dissolved in *aqua regia* and the mass of Ru and Pt ratio from a sample of a known total mass was obtained by using inductively coupled plasma (ICP). Then, the Ru packing density was obtained from the formula

$$\theta_{Ru} = \frac{m_{Ru}}{m_{Pt}} \cdot \frac{N_A}{S \cdot \Gamma_{Pt} \cdot M_{Ru}}, \qquad [1]$$

where θ_{Ru} is the ruthenium packing density; m_{Ru} and m_{Pt} one is the mass of ruthenium and platinum, respectively (from ICP, in grams); N_A is the Avogadro constant; S is the specific surface area of the catalyst, in $cm^2\ g^{-1}$ (see above); Γ_{Pt} is the number of Pt sites per cm^2 (also as above), and M_{Ru} is the atomic mass of Ru. The ruthenium packing density varied from 0.15 to 0.65.

Figure 1 shows cyclic voltammetric (CV) profiles obtained for a clean Pt nanoparticle surface (solid line) and for the ruthenium decorated Pt nanoparticles at the Ru packing density from 0.2 to 0.4. The CV for the Johnson & Matthey Pt/Ru black is shown in the figure inset. In order to obtain the Ru decorated surfaces in the ruthenium density range specified above, four spontaneous depositions were made, and four respective voltammetric curves are shown (Fig. 1). In all cases, the current density is given with respect to the real surface area of the catalyst, as described above. For each spontaneous deposition, the Ru packing density was obtained, and the increase in the Ru packing density after each deposition cycle can easily be deduced from the systematic increase in the charge in double layer range of the Pt/Ru electrode (18). The latter is due to the redox-type transitions between different oxidation states of surface ruthenium occurring in the broad potential range (19). It is interesting to notice that the change in the voltammetric morphology upon Ru deposition in the hydrogen range (Fig. 1) vs that obtained with clean platinum is much less than the corresponding difference between the clean platinum and the Pt/Ru alloy electrode (Fig. 1 inset). Neither does the increase in ruthenium packing contributes to a significant modification of the hydrogen deposition charge. Obviously, hydrogen may adsorb on top of Ru deposited on platinum, although the issue if hydrogen can or cannot be adsorbed on Ru electrodes is still unclear (20, 21). In such a case, reduced hydrogen adsorption on the Pt/Ru alloy surfaces (Fig. 1 inset) is due to the presence of some amount of surface and/or subsurface ruthenium oxide (22), onto which hydrogen is not adsorbed (23). Finally, monatomic Ru islands on the Pt surface can be transparent to protons undergoing the discharge reaction to atomic hydrogen, and hydrogen adsorption may occur underneath the Ru adlayer, the concept that needs to be developed further.

Typical current–time curves for methanol electrooxidation measured after admitting methanol to the cell at 0.3 V are shown in Fig. 2. The decay in the current was observed for 24 h, which secured complete steady-state behavior. It is seen that the clean nanoparticle Pt electrode produces a very small methanol oxidation current due to severe CO poisoning (3) and that the Pt/Ru surfaces display much higher activities. Notice that the 0.4 and 0.5 packing densities of ruthenium on platinum represent the maximum methanol oxidation activity at 0.3 and 0.4 V, respectively, which is shown more explicitly in Fig. 3. This figure also contains current densities for the commercial 50 : 50 Johnson & Matthey catalyst; see open circle data points. The data points are artificially extended using dashed lines toward lower and higher ruthenium packing density to provide baselines for assessment of the current density difference between the decorated and commercial catalysts. *The two decorated Pt/Ru catalysts at 0.3 and 0.4 V, respectively, surpass of the Johnson & Matthey catalyst approximately by a factor of 2*—the main observation of this report—and there is only a small change in the activity maximum on the current vs the Ru packing density curve with the electrode potential.

Notably, while we demonstrate the superior activity of the ruthenium-decorated platinum material vs the industrial benchmark catalyst, we do not claim that we have produced a more active practical catalyst, since the activity of the commercial catalyst per gram of the catalyst is much higher than that of the decorated platinum. The activity here is referenced to the current density per real Pt surface area or to turnover frequency (the number of methanol molecules reacted to carbon dioxide per second, per surface site (24)), and not to the mass of platinum used. The difference between the two catalysts may also be due to particle size effects, as pointed out in Discussion.

After the current became stabilized at 0.3 V at Ru packing density 0.2, the methanol solution was replaced by a clean supporting electrolyte while the potential was maintained at 0.2 V, which prevented CO oxidation from the surface. CO-stripping voltammetric curves were next recorded for the decorated surfaces and for clean Pt to determine

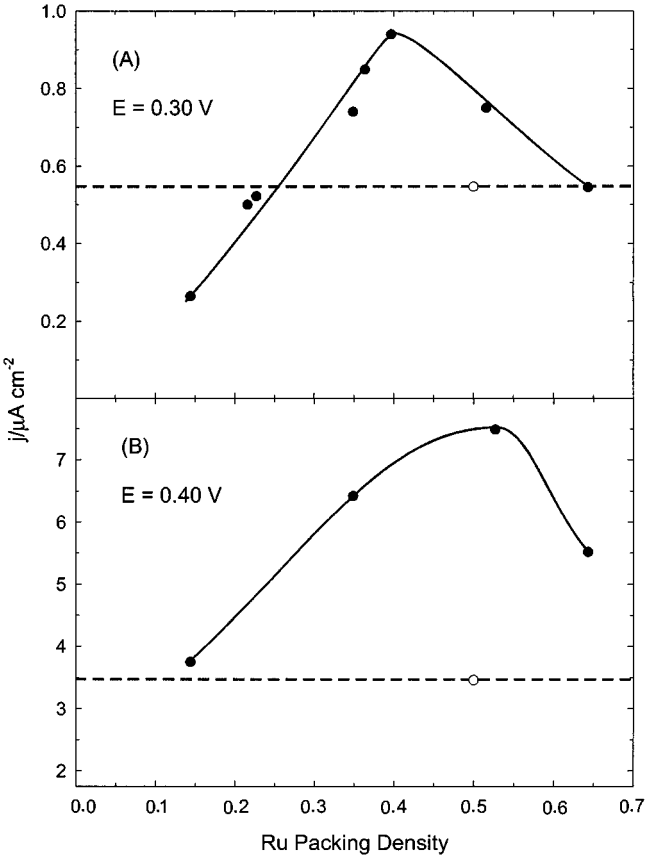

FIG. 3. Dependence of methanol oxidation reactivity of the Pt/Ru catalysts prepared by spontaneous deposition (filled circles) on Ru packing density. Current density is measured after 20 h of oxidation in 0.5 M methanol solution at 0.30 V (A) and 0.40 V (B). (- - ○ - -) is methanol oxidation reactivity of commercial Johnson & Matthey Pt/Ru catalyst under the same experimental conditions as above.

the charge for CO electrooxidation (Fig. 2, inset). There is a significant shift in the main CO electrooxidation feature, which is commented on elsewhere (25). It suffices to say here that the peak position for CO stripping at ca. 0.4 V for the decorated Pt/Ru surface is very similar to that obtained for the commercial Pt/Ru catalyst, as reported previously (12).

DISCUSSION

Let us briefly examine the mechanism of ruthenium enhancement on the Pt/Ru catalysts. As is now well known, steady-state methanol oxidation involves generation of chemisorbed carbon monoxide on the Pt phase of the catalyst in the reaction

$$Pt + CH_3OH \rightarrow Pt\text{–}CO + 4H^+ + 4e^-. \quad [2]$$

It is also broadly acknowledged that methanol decomposition on the Ru phase does not occur (6, 7). To sustain the steady-state current, or the continuous catalytic oxidation process, CO needs to be oxidatively removed from the surface in order to release surface sites needed to sustain the reaction. Clearly, on the bare platinum electrode at the electrode potentials indicated in Fig. 3, the oxidation process is very slow. It is also seen that addition of ruthenium to the Pt catalyst enhances CO removal from the surface since ruthenium promotes CO oxidation to CO_2 (which does not chemisorb on platinum) via the bifunctional mechanism (3, 5–7)

$$Pt\text{–}CO + Ru\text{–}OH \xrightarrow{k} Pt + Ru + CO_2 + H^+ + e^-, \quad [3]$$

where OH symbolizes the oxygen-containing species, or activated water (14), and k is the reaction rate constant. While ligand effects have also been recognized, as mentioned above, they are less pronounced than the bifunctional effects, as demonstrated recently (10). Because of the dissociative character of methanol decomposition (reaction (2)), there is a need for *an ensemble* (26), namely, a specific number of Pt sites where methanol decomposes to fragments. On the previously studied Pt/Ru macroscopic surfaces, the composition that leads to the optimized ensemble size was close to 80–20 Pt–Ru (26, 27). While we do not confirm that the latter ratio holds for the nanoparticle surface (Fig. 3), our data should not be read as contradicting the "ensemble effect." On the alloy, assuming that the surface is made of ruthenium and paltinum only, that is, disregarding ruthenium oxides possibly present on the surface (12), there is enough surface density of sufficiently large Pt aggregates on which methanol decomposes. (The 50 : 50 ratio means only that the manifestation of Pt–Ru pairs on the surface is the most probable, or finding other surface aggregates, Pt_2Ru, Pt_3Ru, etc., is less probable). On the decorated surfaces, there is a static/dynamic distribution of island sizes leaving enough room for the ensemble availability. On the other hand, there is a simultaneous need for maximizing the number of Ru edge sites to secure the most effective CO removal pathway and, as a result of the compromise; the nanostructure surface composition is evidently close to the 50–50 Pt–Ru ratio. Above this ratio, the efficiency of the steady-state methanol oxidant falls, confirming the ensemble effect.

We believe we have a realistic model of steady-state methanol oxidation on a platinum nanoparticle decorated by ruthenium under spontaneous deposition conditions (11, 16, 28, 29). As in electrolysis (30, 31), the spontaneous deposition leads to formation of nanosized ruthenium islands of approximately monoatomic height, with the two-dimensional distribution insensitive to the presence of steps or defects on the surface. Assuming that these previous STM data obtained with smooth single crystal electrodes can be transferred to the surface of a 10-nm nanoparticle, we visualize a cubooctahedral Pt template covered by

protruded two-dimensional nanosized islands, with clearly defined Ru island edges on Pt. From the STM data (16, 29), we may deduce that the island structure is oblivious to cubooctahedral edges, and from voltammetry we conclude that smooth decorated surfaces (32) and 10-nm decorated Pt nanoparticles (25) have very similar electrochemical properties. On the nanoparticle surface, therefore, the active site where CO_2 is formed from CO (from methanol decomposition) is also the edge of the ruthenium island (16, 28–31), with the island interiors inactive to methanol decomposition. As demonstrated in Ref. (31), CO molecules are transferred from methanol decomposition on Pt sites to Ru islands via surface diffusion and are oxidized according to reaction (3). The mobility of CO on a platinum electrode has already been confirmed (33), and ruthenium addition is bound to accelerate this mobility (25).

It is more difficult to explain why the decorated catalyst is more active (in terms of the current density or turnover frequency) than the alloy catalyst. Notice that two catalysts with a similar ratio of platinum to ruthenium ratios are compared. The difference between the catalyst activities cannot therefore be assigned to nominal differences in the density of reactive surface sites. Metal NMR data indicate that the change in the size of platinum nanoparticles down to 1 nm does not change electronic properties, that is, local densities of states (DOS) of such particles (34, 35). In contrast, commercial carbon support affects the DOS (36) and the catalyst activity toward methanol oxidation (37). Since our particles are unsupported, we do not expect that particle size matters in the reactivity change, although this needs to be tested for Pt/Ru. What we see instead is that there is a big difference between the two catalysts in hydrogen adsorption properties—in particular a partial disappearance of high-energy hydrogen on the alloy (Fig. 1). Such disappearance may be correlated, at least formally, to the activity difference in methanol oxidation: the alloy catalyst has a reduced hydrogen stripping potential, certainly from hydronium ion, and very likely from methanol (in reaction (2)). If this is so, the presence of surface/subsurface ruthenium oxide on the alloy may be detrimental to alloy activity (14) (see above). Finally, we notice that the Ru edge atoms are undercoordinated by ruthenium and/or platinum surface atoms and may be more active for water activation than the Pt/Ru sites on the Pt/Ru alloy. In this sense, the latter surface can be considered homogeneous, made of randomly distributed homogeneous ensembles of Pt and Ru sites on the surface of a Pt/Ru cubooctahedral particle, and the decorated surface is spatially heterogeneous. Here, it is known that water activation and the associated oxidation of pure platinum metal electrodes is much facilitated on stepped surfaces rather than on the terrace like Pt(111) surface (38). This suggests that the Ru edge catalytic properties may in part account for the enhanced reactivity of the decorated material that we observe. It is important to test the latter hypothesis since if it is correct, the designing of methanol (CO) oxidation catalysts to contain a maximized number of edge (step) adatoms on the catalyst surface may be one way of improving the activity of methanol fuel cell catalytic materials.

CONCLUSIONS

On all Pt/Ru surfaces investigated in this report as methanol electrooxidation catalysts, methanol is activated via a C–H bond split on the Pt surface phase, it degrades to chemisorbed CO, water is activated on ruthenium, and CO is oxidized at the oxophilic Ru sites. We have found, however, that the decorated Pt/Ru catalyst fabricated in this project is twice as active (in terms of the current density or turnover frequency) as the commercial Johnson & Matthey catalyst, both of nominally identical Pt : Ru ratios. We have also found that hydrogen adsorption/desorption characteristics on the two catalysts are significantly different, therefore, one possibility to interpret the methanol reactivity difference is to link the two observations together. If this is so, this would assume that the hydrogen stripping capacity of the alloy surface (essential in the dehydrogenation step, reaction (2)), is less than that of the decorated surface. Possible reasons for such a behavior, relating to the role of ruthenium oxide present on the alloy particles at potentials of adsorbed hydrogen and methanol oxidation (12), are discussed above. However, given the paradigm that Ru nanoisland's interiors are inactive to methanol decomposition, we may also conclude that ruthenium atoms present at the edge of Ru nanosized islands display significantly enhanced activity for the CO poison removal in comparison with the Pt/Ru alloy active sites. Since the Pt/Ru mixed metal material is used as an anode in a direct oxidation methanol fuel cell, these interpretations may give one a clue about the optimized structure of high activity catalysts of some specific fuel cell applications.

ACKNOWLEDGMENTS

This work is supported by Department of Energy Grant DEFG02-99ER14993 and by the National Science Foundation under Grant CHE 9985837. J.S-G. is grateful to the "Consellería de Cultura, Educación y Ciencia de la Generalitat Valenciana" for giving him the opportunity of contributing to this project.

REFERENCES

1. EG&G Services, Parsons, Inc., and Science Applications International Corporation "Fuel Cell Handbook," 5th ed. U.S. Department of Energy, Morgantown, WV, 2000; available at http://216.51.18.233/fchandbook.pdf.
2. Gottesfeld, S., and Zawodzinski, T., in "Advances in Electrochemical Science and Engineering" (R. C. Alkire, H. Gerisher, D. M. Kolb, and C. W. Tobias, Eds.), Vol. 5, p. 195. Wiley, New York/VCH, Weinheim/New York, 1997.

3. Hamnett, A., in "Interfacial Electrochemistry: Theory, Experiment, and Applications" (A. Wieckowski, Ed.), p. 843. Dekker, New York, 1999.
4. Franaszczuk, K., Herrero, E., Zelenay, P., Wieckowski, A., Wang, J., and Masel, R. I., *J. Phys. Chem.* **96**, 8508 (1992).
5. Watanabe, M., and Motoo, S., *J. Electroanal. Chem.* **60**, 275 (1975).
6. Markovic, N. M., Gasteiger, H. A., Ross, Jr., P. N., Jiang, X., Villegas, I., and Weaver, M. J., *Electrochim. Acta* **40**, 91 (1995).
7. Gasteiger, H. A., Markovic, N., Ross, Jr., P. N., and Cairns, E. J., *J. Phys. Chem.* **97**, 12,020 (1993).
8. Iwasita, T., Nart, F. C., and Vielstich, W., *Ber. Bunserges. Phys. Chem.* **94**, 1030 (1990).
9. Frelink, T., Visscher, W., and van Veen, J. A. R., *Langmuir* **12**, 3702 (1996).
10. Lu, C., and Masel, R., *J. Phys. Chem. B*, in press.
11. Chrzanowski, W., and Wieckowski, A., *Langmuir* **13**, 5974 (1997).
12. Crown, A., Kim, H., Lu, G. Q., de Moraes, I. R., Rice, C., and Wieckowski, A., *J. New Mater. Electrochem. Syst.* **3**, 275 (2000).
13. Waszczuk, P., Wieckowski, A., Zelenay, P., Gottesfeld, S., Coutanceau, C., Léger, J.-M., and Lamy, C., *J. Electroanal. Chem.*, in press.
14. Kim, H., Tremiliosi-Filho, G., Haasch, R., Moraes, I., and Wieckowski, A., *Surf. Sci. Lett.* **474**, L203 (2001).
15. Angerstein-Kozlowska, H., in "Comprehensive Treatise of Electrochemistry" (E. Yeager, J. O'M. Bockris, and S. Sarangapani, Eds.), Vol. 9, p. 15. Plenum, New York, 1984.
16. Crown, A., Moraes, I. R., and Wieckowski, A., *J. Electroanal. Chem.* **500**, 333 (2001).
17. Herrero, E., Chrzanowski, W., and Wieckowski, A., *J. Phys. Chem.* **99**, 10423 (1995).
18. Chrzanowski, W., Kim, H., and Wieckowski, A., *Catal. Letters* **50**, 69 (1998).
19. Conway, B. E., *Prog. Surf. Sci.* **49**, 331 (1995).
20. Wang, W. B., Zei, M. S., and Ertl, G., *Phys. Chem. Chem. Phys.* **3**, advance article, 2001.
21. Wang, J. X., Marinkovic, N. S., Zajonz, H., Ocko, B. M., and Adzic, R. R., *J. Phys. Chem. B* **105**, 2809 (2001).
22. Rolison, D. R., Hagans, P. L., Swider, K. E., and Long, J. W., *Langmuir* **15**, 774 (1999).
23. Chu, Y. S., Lister, T. E., Cullen, W. G., You, H., and Nagy, Z., *Phys. Rev. Lett.* **86**, 3364 (2001).
24. Chrzanowski, W., and Wieckowski, A., in "Interfacial Electrochemistry: Theory, Experiment and Applications" (A. Wieckowski, Ed.), p. 950. Dekker, New York, 1999.
25. Tong, Y. Y., Kim, H. S., Babu, P. K., Waszczuk, P., Oldfield, E., and Wieckowski, A., submitted for publication.
26. Gasteiger, H. A., Markovic, N., Ross, P. N., Jr., and Cairns, E. J., *Electrochim. Acta* **39**, 1825 (1994).
27. Chrzanowski, W., and Wieckowski, A., *Langmuir* **14**, 1967 (1998).
28. Herrero-Rodriguez, E., Feliu, J. M., and Wieckowski, A., *Langmuir* **15**, 4944 (1999).
29. Crown, A., and Wieckowski, A., *Phys. Chem. Chem. Phys.* **3**, advance article (2001).
30. Friedrich, K. A., Geyzers, K.-P., Linke, U., Stimming, U., and Stumper, J., *J. Electroanal. Chem.* **402**, 123 (1996), page 126.
31. Friedrich, K. A., Geyzers, K.-P., Marmann, A., Stimming, U., and Vogel, R., *Z. Phys. Chem.* **208**, 137 (1999).
32. Massong, H., Wang, H. S., Samjeske, G., and Baltruschat, H., *Electrochem. Acta* **46**, 701 (2000).
33. Day, J. B., Vuissoz, P.-A., Oldfield, E., Wieckowski, A., and Ansermet, J. P., *J. Am. Chem. Soc.* **118**, 13,046 (1996).
34. Van Der Klink, J. J., *Z. Phys.* **12**, 327 (1989).
35. Tong, Y. Y., Billy, J., Renouprez, A. J., and Van Der Klink, J. J., *J. Am. Chem. Soc.* **119**, 3929 (1997).
36. Tong, Y. Y., Belrose, C., Godbout, N., Wieckowski, A., and Oldfield, E., *J. Am. Chem. Soc.* **121**, 2996 (1999).
37. Mukerjee, S., and Mcbreen, J., *J. Electroanal. Chem.* **448**, 163 (1998).
38. Herrero, E., Franaszczuk, K., and Wieckowski, A., *J. Phys. Chem.* **98**, 5074 (1994).